# THE LONGITUDINAL DYNAMIC CORRELATION AND DYNAMIC SUSCEPTIBILITY OF THE ISOTROPIC XY-MODEL ON THE 1D ALTERNATING SUPERLATTICE§

J. P. de Lima

Departamento de Física da Universidade Federal do Piauí Campus Ministro Petrônio Portela, 64049-550 Teresina, Piauí, Brazil and

L. L. Gonçalves\*

Departamento de Física da Universidade Federal do Ceará Campus do Pici, C.P. 6030, 60451-970 Fortaleza, Ceará, Brazil

#### Abstract

The dynamic susceptibility  $\chi_Q^{zz}(\omega)$  of the isotropic XY-model (s=1/2) on the alternating superlattice (closed chain) in a transverse field h is obtained exactly at arbitrary temperatures. It is determined from the results obtained for the dynamic correlations  $\langle S_{jn}^z(t)S_{lm}^z(0)\rangle$ , which have been calculated by introducing the generalized Jordan-Wigner transformation, by using Wick's theorem and by reducing the problem to a diagonalization of a finite matrix. The static properties are also reobtained within this new formalism and all exact results are determined for arbitrary temperatures. Explicit results are obtained numerically in the limit T=0, where the critical behaviour occurs. A detailed analysis is presented for the behaviour of the static susceptibility  $\chi_O^{zz}(0)$ , as a function of the transverse field h, and for the frequency dependency of the dynamic susceptibility  $\chi_Q^{zz}(\omega)$ . It is also shown, in this temperature limit, that within the magnetization plateaus which correspond to the different phases, even when the induced magnetization is not saturated, the effective  $\sum_{n;m\in cell:\; j;l}S_{jn}^z(t)S_{lm}^z(0)>$  , is time independent, which dynamic correlation, < constitutes an unexpected result.

E-mail address: lindberg@fisica.ufc.br (L. L. Gonçalves)

PACS: 05.90.+m;75.10Jm

Keywords: XY model; dynamic susceptibility; dynamic correlation; one-dimensional superlattice.

<sup>§</sup> A preliminary version of this work has been presented at STATPHYS 21, July 2001, Cancun, Mexico.

<sup>\*</sup>Corresponding author.

## 1. Introduction

The homogeneous one-dimensional XY-model introduced by Lieb et al.[1] has been object of many studies. Its importance comes mainly from the fact that it is among the few many-body problems which can be solved exactly. Although the static and dynamic properties of the general homogeneous model have been studied since its introduction (see e.g. Ref. [2] and references therein), the study of the inhomogeneous periodic model has been restricted to the alternating chain [3-5]. Only recently have more general inhomogeneous models been object of study, namely, the alternating superlattice [6-8] and the inhomogeneous periodic model composed of inhomogeneous segments of finite length [9,10]. The results of these papers have been restricted to the static properties of the isotropic model and up to this date, to the best of our knowledge, no results have been obtained for the dynamic properties of these models.

In this paper we study the dynamic properties of the isotropic model on the alternating one-dimensional superlattice. The dynamic properties are restricted to the longitudinal direction and they correspond to an extension of our previous results [6-8]. In section 2 we present the solution of the model and the basic results. In section 3 we obtain the dynamic correlations in the field direction and in section 4 the longitudinal dynamic susceptibility. Finally in section 5 we present the results and the main conclusions.

### 2. The model: basic results

We consider the isotropic XY model on the one-dimensional alternating superlattice, which we have been able to solve exactly[7]. The superlattice consists of N cells, composed of two subcells, A and B, with  $n_A$  and  $n_B$  sites, respectively. The l-th unit cell is shown in Fig.1, and the distance s between two consecutive sites is taken equal to one.

If we assume periodic boundary conditions for a chain with N cells, the Hamiltonian of the XY-model [7] can be written in the form

$$H = -\frac{1}{2} \sum_{l=1}^{N} \left\{ \left[ \sum_{m=1}^{n_{A}-1} J_{A} S_{l,m}^{A^{+}} S_{l,m+1}^{A^{-}} + \sum_{m=1}^{n_{B}-1} J_{B} S_{l,m}^{B^{+}} S_{l,m+1}^{B^{-}} + J \left( S_{l,n_{A}}^{A^{+}} S_{l,1}^{B^{-}} + S_{l,n_{B}}^{B^{+}} S_{l+1,1}^{A^{-}} \right) + h.c. \right] + \sum_{m=1}^{n_{A}} 2h_{A} S_{l,m}^{A^{Z}} + \sum_{m=1}^{n_{B}} 2h_{B} S_{l,m}^{B^{Z}} \right\},$$

$$(1)$$

where l identifies the cell,  $S^{\pm} = S^x \pm i S^y$ , J is the exchange parameter between spins at the interfaces,  $J_A(J_B)$  the exchange parameter between spins within the subcell A(B), and  $h_A(h_B)$  is the transverse field within the subcell A(B). The spin operators can be expressed in terms of fermion operators using the generalized Jordan-Wigner transformation [6]

$$S_{l,m}^{A^{+}} = \exp\left\{i\pi \sum_{n=1}^{l-1} \sum_{r=1}^{n_{A}} a_{n,r}^{\dagger} a_{n,r} + i\pi \sum_{r=1}^{m-1} a_{l,r}^{\dagger} a_{l,r} + i\pi \sum_{n=1}^{l-1} \sum_{r=1}^{n_{B}} b_{n,r}^{\dagger} b_{n,r}\right\} a_{l,m}^{\dagger} ,$$
(2)

$$S_{l,m}^{B^{+}} = \exp\left\{i\pi \sum_{n=1}^{l} \sum_{r=1}^{n_{A}} a_{n,r}^{\dagger} a_{n,r} + i\pi \sum_{r=1}^{m-1} b_{l,r}^{\dagger} b_{l,r} + i\pi \sum_{n=1}^{l-1} \sum_{r=1}^{n_{B}} b_{n,r}^{\dagger} b_{n,r}\right\} b_{l,m}^{\dagger} ,$$
(3)

and, by introducing this transformation, the Hamiltonian can be written in the form

$$H = -\frac{1}{2} \sum_{l=1}^{N} \left\{ \sum_{m=1}^{n_{A}-1} J_{A} a_{l,m}^{\dagger} a_{l,m+1} + \sum_{m=1}^{n_{B}-1} J_{B} b_{l,m}^{\dagger} b_{l,m+1} + \right. \\ \left. + J \left( a_{l,n_{A}}^{\dagger} b_{l,1} + b_{l,n_{B}}^{\dagger} a_{l+1,1} \right) + h.c. \right. \\ \left. + \sum_{m=1}^{n_{A}} 2h_{A} \left( a_{l,m}^{\dagger} a_{l,m} - 1 \right) + \sum_{m=1}^{n_{B}} 2h_{B} \left( b_{l,m}^{\dagger} b_{l,m} - 1 \right) \right\} + \Phi, \quad (4)$$

where a's and b's are fermion operators, and  $\Phi$ , given by

$$\Phi = \frac{J}{2} \left( b_{N,n_B}^{\dagger} a_{1,1} + h.c. \right) \exp \left[ i\pi \left( \sum_{l=1}^{N} \sum_{r=1}^{n_A} a_{l,r}^{\dagger} a_{l,r} + \sum_{l=1}^{N} \sum_{r=1}^{n_B} b_{l,r}^{\dagger} b_{l,r} \right) \right] ,$$
(5)

is a boundary term which will be neglected. As it has been shown [11], this boundary term, in the thermodynamic limit, does not affect the excitation spectrum, the static properties of the system, nor the dynamic correlation function in the field direction. Introducing the Fourier transforms [8],

$$A_{Q,m} = \frac{1}{\sqrt{N}} \sum_{l} \exp(-iQdl) a_{l,m} , \qquad (6)$$

$$B_{Q,m} = \frac{1}{\sqrt{N}} \sum_{l} \exp(-iQdl) b_{l,m} \qquad , \tag{7}$$

where  $Q = 2\pi n/Nd$ , n = 1, 2, ..., N, and  $d = n_A + n_B$  is the size of the cell, the Hamiltonian can be written as

$$H = \sum_{Q} H_Q + N \left( \frac{n_A h_A + n_B h_B}{2} \right) \qquad , \tag{8}$$

where  $H_Q$  is given by

$$H_{Q} = -\sum_{m=1}^{n_{A}} h_{A} A_{Q,m}^{\dagger} A_{Q,m} - \sum_{m=1}^{n_{B}} h_{B} B_{Q,m}^{\dagger} B_{Q,m} - \sum_{m=1}^{n_{A}-1} \left( \frac{J_{A}}{2} A_{Q,m}^{\dagger} A_{Q,m+1} + h.c \right) - \sum_{m=1}^{n_{B}-1} \left( \frac{J_{B}}{2} B_{Q,m}^{\dagger} B_{Q,m+1} + h.c \right) - \frac{J}{2} \left[ A_{Q,n_{A}}^{\dagger} B_{Q,1} + B_{Q,n_{B}}^{\dagger} A_{Q,1} e^{-iQd} + h.c. \right] + N \frac{(n_{A} h_{A} + n_{B} h_{B})}{2}.$$
 (9)

We can also write H in the form

$$H = \sum_{Q} V_Q^{\dagger} \mathbf{T}(Q) V_Q, \tag{10}$$

where

$$V_Q^{\dagger} = \left( A_{Q,1}^{\dagger}, ..., A_{Q,n_A}^{\dagger}, B_{Q,1}^{\dagger}, ..., B_{Q,n_B}^{\dagger} \right) \tag{11}$$

and  $\mathbf{T}(Q)$  is a matrix of dimension  $d \times d$  which represents the quadratic Hamiltonian  $H_Q$ . Since  $[H_Q, H_{Q'}] = 0$ , the diagonalization of the Hamiltonian is reduced to the diagonalization of  $H_Q$ , which can be written as a free fermion system

$$H_Q = \sum_k E_{Qk} \xi_{Q,k}^{\dagger} \xi_{Q,k}, \tag{12}$$

where  $E_{Qk}$  are the diagonal elements of  $U_Q \mathbf{T}_Q U_Q^{\dagger}$ , and  $U_Q$  is the unitary transformation which diagonalizes  $H_Q$ , which is determined numerically. The

energy spectrum presents d branches and, by using the unitary transformation  $U_Q$ , we can express the fermion operators a's and b's in terms of the  $\xi's$ , as

$$A_{Q,m} = \sum_{k} u_{Q,m,k} \xi_{Q,k}, \tag{13}$$

$$B_{Q,m} = \sum_{k} u_{Q,n_A+m,k} \xi_{Q,k}, \tag{14}$$

$$a_{l,m} = \frac{1}{\sqrt{N}} \sum_{Q,k} \exp(iQdl) u_{Q,m,k} \xi_{Q,k},$$
 (15)

$$b_{l,m} = \frac{1}{\sqrt{N}} \sum_{Q,k} \exp(iQdl) u_{Q,n_A+m,k} \xi_{Q,k},$$
 (16)

where  $u_{Q,k,j}$  are defined as

$$\mathbf{T}_{Q} \begin{bmatrix} u_{Q,k,1} \\ \dots \\ u_{Q,k,n_{A}} \\ u_{Q,k,n_{A}+1} \\ \dots \\ u_{Q,k,n_{A}+n_{B}} \end{bmatrix} = E_{Qk} \begin{bmatrix} u_{Q,k,1} \\ \dots \\ u_{Q,k,n_{A}} \\ u_{Q,k,n_{A}+1} \\ \dots \\ u_{Q,k,n_{A}+n_{B}} \end{bmatrix}.$$
 (17)

The general solution of this equation is determined numerically, although analytical solutions can be found for some special cases. For instance for  $n_A = n_B = 2$ ,  $h_A = h_B = h$ , we can express explicitly the solution in the form

$$\omega_Q = -h \pm \frac{1}{\sqrt{2}} \sqrt{c \pm \sqrt{g(Qd)}} \qquad , \tag{18}$$

where

$$c \equiv \frac{J^2}{2} + \frac{1}{4} \left( J_A^2 + J_B^2 \right) \qquad , \tag{19}$$

$$g(Qd) \equiv \frac{1}{2}J^2J_AJ_B\cos(Qd) + \frac{J^2}{4}(J_A^2 + J_B^2) + \frac{1}{16}(J_A^2 - J_B^2)^2$$
. (20)

As it has already been shown [7], the effect of a homogeneous field,  $h_A = h_B = h$ , is to shift the zero field spectrum. For the special case shown above this can also be shown directly from eq.(18) and, consequently, the existence of a mode of zero energy will depend on the strength of the field.

In passing, we would like to note that the spectrum can also be calculated exactly by using the position space renormalization group approach [12], and approximately by using a transfer matrix method [13]. Although the latter is an approximate method, we have shown that it reproduces numerically the exact result.

Within the formalism introduced above we can obtain easily all the thermodynamic properties of the system. Then, we can express the internal energy U in the form

$$U = \sum_{Q,k} E_{Qk} \langle n_{Qk} \rangle, \text{ with } \langle n_{Qk} \rangle = \frac{1}{1 + e^{\beta E_{Qk}}},$$
 (21)

where  $\beta = 1/k_BT$ ,  $k_B$  is the Boltzmann constant and T, the absolute temperature, and from this expression we obtain immediately the specific heat C

$$C = \frac{1}{k_B T^2} \sum_{Q,k} E_{Qk} e^{\beta E_{Qk}} \left\langle n_{Qk} \right\rangle^2. \tag{22}$$

The induced magnetization per site and cell, which is defined as [7],

$$\langle S_{cel}^z \rangle = \frac{1}{N(n_A + n_B)} \left[ \sum_{l=1}^N \left( \sum_{m=1}^{n_A} \left\langle S_{l,m}^{A^z} \right\rangle + \sum_{m=1}^{n_B} \left\langle S_{l,m}^{B^z} \right\rangle \right) \right], \tag{23}$$

can also be written in the form

$$\langle S_{cel}^z \rangle = \frac{1}{N(n_A + n_B)} \left[ \sum_{Qk} \langle n_{Qk} \rangle \right] - \frac{1}{2},$$
 (24)

and from this expression, by making the identification  $h_A = h_B \equiv h$ , we can obtain the isothermal susceptibility,  $\chi_T^{zz} = \frac{\partial}{\partial h} \langle S_{cel}^z \rangle$ , which is given by

$$\chi_T^{zz} = \frac{\beta}{N(n_A + n_B)} \sum_{Qk} \langle n_{Qk} \rangle^2 \exp(\beta E_{Qk}). \tag{25}$$

## 3. The Dynamic Two-Spin Correlation Function in the Field Direction

The dynamic two-spin correlation function,  $\langle S_{j,m}^{A^z}(t)S_{j+R,n}^{A^z}(0)\rangle$ , can be easily obtained by writing explicitly the time-evolution of the operator  $S_{j,m}^{A^Z}(t)$ . This is obtained by using eqs. (2) and (15), which gives

$$S_{j,m}^{A^{Z}}(t) = \frac{1}{N} \sum_{Q,k,Q',k'} \left[ \exp\left(-i(Q-Q')dj\right) \exp\left(i(E_{Qk} - E_{Q'k'})t\right) \right.$$
$$\left. u_{Q,k,m}^{*} u_{Q',k',m} \xi_{Q,k}^{\dagger} \xi_{Q',k'} \right] - \frac{1}{2}, \tag{26}$$

and from this we can write

$$\left\langle S_{j,m}^{A^{z}}(t)S_{j+R,n}^{A^{z}}(0)\right\rangle = \left\langle \left(\frac{1}{N}\sum_{Q,k,Q',k'}\exp\left(-i(Q-Q')dj\right)\times\right.\right. \\ \left. \times \exp(i(E_{Qk}-E_{Q'k'})t)u_{Q,k,m}^{*}u_{Q',k',m}\xi_{Q,k}^{\dagger}\xi_{Q',k'}-\frac{1}{2}\right)\times \\ \left. \times \left(\frac{1}{N}\sum_{Q,k,Q',k'}\exp\left(-i(Q-Q')dl\right)u_{Q,k,n}^{*}u_{Q',k',n}\xi_{Q,k}^{\dagger}\xi_{Q',k'}-\frac{1}{2}\right)\right\rangle.$$
 (27)

By using Wick's theorem we obtain

$$\left\langle S_{j,m}^{A^{z}}(t)S_{j+R,n}^{A^{z}}(0)\right\rangle =$$

$$\left(\frac{1}{N}\sum_{Q,k}\exp\left(-iQRdl\right)\exp(iE_{Qk}t)u_{Q,k,m}^{*}u_{Q,k,m}u_{Q,k,m}\left\langle n_{Qk}\right\rangle\right)\times$$

$$\left(\frac{1}{N}\sum_{Q,k}\exp\left(iQRdl\right)\exp(-iE_{Qk}t)u_{Q,k,n}^{*}u_{Q,k,n}\left(1-\langle n_{Qk}\rangle\right)\right)+$$

$$\left(\frac{1}{N}\sum_{Q,k}u_{Q,k,m}u_{Q,k,m}^{*}\left\langle n_{Qk}\right\rangle\right)\times\left(\frac{1}{N}\sum_{Q,k}u_{Q,k,n}u_{Q,k,n}^{*}\left\langle n_{Qk}\right\rangle\right)+$$

$$-\frac{1}{2}\frac{1}{N}\sum_{Q,k}u_{Q,k,m}u_{Q,k,m}^{*}\left\langle n_{Qk}\right\rangle-\frac{1}{2}\frac{1}{N}\sum_{Q,k}u_{Q,k,n}u_{Q,k,n}^{*}\left\langle n_{Qk}\right\rangle+\frac{1}{4},\quad(28)$$

which can be determined numerically.

We can also obtain the dynamic correlation between average cell spin operators,  $\tau_L^z$ , defined as

$$\tau_l^z = \frac{1}{(n_A + n_B)} \left( \sum_{m=1}^{n_A} S_{l,m}^{A^z} + \sum_{m=1}^{n_B} S_{l,m}^{B^z} \right), \tag{29}$$

which satisfy the equality  $\langle \tau_l^z \rangle = \langle S_{cel}^z \rangle$ . Therefore, by using eqs. (28) and (29), we can determine the dynamic correlation function  $\langle \tau_l^z(t) \tau_{l+R}^z(0) \rangle$  by expressing it in terms of dynamic correlations between site spins and it can be writen in the form

$$\left\langle \tau_{l}^{z}(t)\tau_{l+R}^{z}(0)\right\rangle = \left[\frac{1}{N\left(n_{A}+n_{B}\right)}\sum_{Q,k}\left(\langle n_{Qk}\rangle - \frac{1}{2}\right)\right]^{2} + \left(\frac{1}{N\left(n_{A}+n_{B}\right)}\right)^{2}\left(\sum_{Q,k}\exp\left(-iQRdl\right)\exp(iE_{Qk}t)\left\langle n_{Qk}\right\rangle\right) \times \left(\sum_{Q,k}\exp\left(iQRdl\right)\exp(-iE_{Qk}t)\left(1-\langle n_{Qk}\rangle\right)\right). \tag{30}$$

## 4. The Longitudinal Dynamic Susceptibility

The dynamic susceptibility  $\chi_Q^{zz}(\omega)$  can be determined by introducing the spatial and temporal Fourier transforms

$$\left\langle \tau_{Q}^{z}(t)\tau_{-Q}^{z}(0)\right\rangle =\sum_{R}\exp(-iQR)\left\langle \tau_{l}^{z}(t)\tau_{l+R}^{z}(0)\right\rangle ,\tag{31}$$

and

$$\left\langle \tau_Q^z \tau_{-Q}^z \right\rangle_{\omega} = \frac{1}{2\pi} \int_{-\infty}^{\infty} \exp(i\omega t) \left\langle \tau_Q^z(t) \tau_{-Q}^z(0) \right\rangle dt, \tag{32}$$

and by using eq. (30) we can write

$$\left\langle \tau_{Q}^{z} \tau_{-Q}^{z} \right\rangle_{\omega} = N \delta\left(\omega\right) \delta_{Q,0} \left[ \frac{1}{N\left(n_{A} + n_{B}\right)} \sum_{Q_{1}, k} \left( \langle n_{Q_{1}k} \rangle - \frac{1}{2} \right) \right]^{2} + \frac{1}{N\left(n_{A} + n_{B}\right)^{2}} \sum_{Q_{1}, k} \delta\left(\omega + E_{Qk} - E_{Q_{1} - Qk}\right) \langle n_{Q_{1}k} \rangle \times \left(1 - \langle n_{Q_{1} - Qk} \rangle\right).$$

$$(33)$$

From this result we can obtain the dynamic susceptibility from the expression [14]

$$\chi_Q^{zz}(\omega) = -2\pi \ll \tau_Q^z; \tau_{-Q}^z >> = -\int_{-\infty}^{\infty} \frac{\left(1 - \exp(\beta\omega)\right) \left\langle \tau_Q^z \tau_{-Q}^z \right\rangle_{\omega'} d\omega'}{\omega - \omega'}, \quad (34)$$

which can be written as

$$\chi_Q^{zz}(\omega) = \frac{1}{N(n_A + n_B)^2} \sum_{Q_1,k} \frac{\langle n_{Q_1k} \rangle - \langle n_{Q_1 - Q_k} \rangle}{\omega + E_{Qk} - E_{Q_1 - Qk}}.$$
 (35)

In the limit  $\omega \to 0, Q \to 0$ , we obtain the isothermal susceptibility as in the uniform model [15].

The real and imaginary parts of  $\chi_Q^{zz}(\omega)$  can be determined from the previous expression by considering  $\chi_Q^{zz}(\omega - i\epsilon)$  in the limit  $\epsilon \longrightarrow 0$ , and from this we obtain explicitly the results

$$\operatorname{Re} \chi_Q^{zz}(\omega) = \frac{1}{N(n_A + n_B)^2} \sum_{Q_1, k} \frac{\langle n_{Q_1 k} \rangle - \langle n_{Q_1 - Q_k} \rangle}{\omega + E_{Qk} - E_{Q_1 - Qk}}$$
(36)

and

$$\operatorname{Im} \chi_{Q}^{zz}(\omega) = \frac{\pi}{N(n_A + n_B)^2} \sum_{Q_1, k} (\langle n_{Q_1 k} \rangle - \langle n_{Q_1 - Q k} \rangle) \delta(\omega + E_{Qk} - E_{Q_1 - Qk}).$$
(37)

## 5. Results and Conclusions

The results for J=1,  $J_A=2$ ,  $J_B=3$ ,  $h_A=h_B=h$  and  $n_A=n_B=2$ , at T=0 are shown in Figs. 2, 4, 5, 8, 10 and 12. For the same interaction parameters and  $n_A=2$ ,  $n_B=3$ , the results are shown in Figs. 3, 6, 7, 9, 11 and 13.

In Figs. 2 and 3 we present the magnetization  $\langle \tau_l^z \rangle$  and the isothermal susceptibility  $\chi_T^{zz}$  as functions of the field. In these cases, as expected, we have four and five critical fields respectively, associated to the quantum transitions induced by the field and the isothermal susceptibility diverges at these points. In the first case  $(n = n_A + n_B, \text{ even})$  there is a plateau at zero magnetization, whereas in the second one  $(n = n_A + n_B, \text{ odd})$  the magnetization plateaus are at non-zero values. These results suggest that these plateaus, which are associated to the gaps in the energy spectrum [7], can also be related to the cluster spin states in a representation where the effective spin  $\tau_l^z$  is diagonal [10].

In Figs. 4-7 we present the real and imaginary parts of the dynamic correlation function  $\langle \tau_l^z(t)\tau_{l+R}^z(0)\rangle$ , as a function of time t, for R=1. For n=4, Figs. 4 and 5, the results are presented for three different values of the field, namely,  $h=h_{jc}$  and  $h=h_{jc}+\varepsilon$  ( $\varepsilon=0.001,\,0.01$ ), where j=1,3 respectively for each figure. For n=5, Figs.6 and 7, the results are also presented for three different values of the field, namely,  $h=h_{jc}$  and  $h=h_{jc}-\varepsilon$  ( $\varepsilon=0.001,\,0.01$ ), where j=1,3 respectively for each figure. In all cases, the imaginary part of the correlation goes to zero as we approach the magnetization plateaus, and the real part tends to the square of the magnetization  $\langle \tau_l^z \rangle$ . These results show that within the plateaus, although  $\langle S_{j,m}^{A(B)^z}(t)S_{j+R,n}^{A(B)^z}(0)\rangle$  are not constant, the field does not induce any quantum fluctuation on the correlation  $\langle \tau_l^z(t)\tau_{l+R}^z(0)\rangle$ . This means that the system, although not saturated, is in a frozen effective spin state.

In Figs. 8 and 9 we show the static correlation function  $\langle \tau_j^z \ \tau_{j+R}^z \rangle$  as a function of R, the distance between cells, at T=0, and three different values of the field. The correlation shows an oscillatory behaviour which is present for any value of the field outside the plateaus, with increasing period as the critical point is approached. On the other hand, at the critical field there is no oscillatory behaviour, which means that the period of the oscillation tends to infinity, and this result is still valid for any value of the field within the plateaus. This is consistent with the scaling form and the analytical continuation proposed for the two-spin correlation function  $\langle S_j^z(0)S_{ln}^z(0)\rangle$  in the homogeneous XY-model [16], where the correlation length is associated to the oscillation period.

We have also verified that for  $h \ge h_{4c}$  (n=4, even) and  $h \ge h_{5c}$  (n=5, odd), since the system is saturated, the dynamic correlation function  $< S_{jn}^{A(B)z}(t)S_{lm}^{A(B)z}(0) > \text{does not depend on time nor field, while in the intermediate plateaus it presents a time dependence which is independent of the value of the field.$ 

The static susceptibility  $\chi_Q^{zz}(0)$ , at T=0, is shown in Figs. 10 and 11 for various wave-vectors and the two different cell sizes. As already pointed out, the susceptibility  $\chi_0^{zz}(0)$  is identical to the isothermal one  $\chi_T^{zz}$  and consequently diverges at the critical points. Also, independently of the wave-vector, the static susceptibility goes to zero within the magnetization plateaus since in this region the spacial modulation of the magnetic field does not induce any fluctuation in the magnetization. The singularities present for the different non-zero wave-vectors are related to the oscillations of the correlation  $\langle \tau_l^z(t)\tau_{l+R}^z(0)\rangle$ , whereas the ones for Q=0 are related to the critical points. As pointed out by Jullien and Pfeuty [17] for the homogeneous model and Lima and Gonçalves for the model on the supperlattice [18], the non-critical singularities can also be associated to the unstable critical points. which appear in the study of the system within the real space renormalization approach.

Finally, in Figs. 12 and 13 we present the real and imaginary parts of the dynamic susceptibility,  $\chi_q^{zz}(\omega)$ , at T=0, for values of the field close to critical ones and outside the plauteaus, and the same parameters of the previous figures. As expected, for a given wave-vector, the bandwidth of the imaginary part of the response depends on the field strength and on the size of the cell and there are no infinite singularities. Also as expected, to the finite discontinuities at the band edges of the imaginary part correspond divergences in the real part. It should be noted that for values of the field within the plateaus the response goes to zero for any non-zero wave-vector.

#### Acknowledgements

The authors would like to thank the Brazilian agencies CNPq, Capes and Finep for the partial financial support.

## References

- [1] E. Lieb, T. Schultz, D. Mattis, Ann. Phys. (NY) 16 (1961) 407.
- [2] J. Stolze, A. Nopert, G. Müller, Phys. Rev. B 52 (1995) 4319 and references therein.
- [3] V. M. Kontorovich, V. M. Tsurkenik, Sov. Phys. JEPT 26 (1968) 687.
- [4] J. H. H. Perk, H. W. Capel, M. J. Zuilhof, Physica A 81 (1975) 319.
- [5] J. H. H. Perk, Th. J. Siskens, H. W. Capel, Physica A 89 (1977) 304.
- [6] J. P. de Lima, L.L. Gonçalves, J. Magn. & Magn. Mater. 140-144, 1606 (1995)
- [7] J. P. de Lima, L. L. Gonçalves, J. Magn. & Magn. Mater. 206, (1999) 135 and references therein.
- [8] F. F. Barbosa Filho, J. P. de Lima, L. L. Gonçalves, J. Magn. & Magn. Mater. 226-230 (2001) 638.
- [9] O. Derzhko, J. Richter, O. Zaburannyi, Physica A 282 (2000) 495.
- [10] O. Derzhko, J. Richter, O. Zaburannyi, J. Magn. & Magn. Mater. 222 (2000) 207.
- [11] L. L. Gonçalves, Theory of Properties of Some One-Dimensional Systems,
  - (D.Phil.Thesis, University of Oxford, 1977).
  - [12] J. P. de Lima, L.L. Gonçalves, Mod. Phys. Lett. **B22** (1996) 1077.
- [13] L. L. Gonçalves, J.P. de Lima, J. Phys.: Condens. Matter **9** (1997) 3447.
  - [14] D. N. Zubarev, Sov. Phys. Usp. 3 (1960) 320.
  - [15] S. Katsura, T. Horiguchi, M. Suzuki, Physica **46** (1970) 67.
  - [16] J. P. de Lima, L.L. Gonçalves, Mod. Phys. Lett. B 14&15 (1997) 871.
  - [17] R. Jullien, P. Pfeuty, Phys. Rev **B19** (1979) 4646.
  - [18] J. P. de Lima, L. L. Gonçalves, Mod. Phys. Lett. **B22** (1996) 1077.

## Figure Captions

- Fig.1-Unit cell of the alternating superlattice.
- **Fig. 2-** Average magnetization per unit cell (a) and the susceptibility in the field direction (b) as functions of the field, for  $n_A = n_B = 2$ , J = 1,  $J_A = 2$ ,  $J_B = 3$ , and  $h_A = h_B = h$ , at T = 0. The critical fields are  $h_{c1} \cong 0.691$ ,  $h_{c2} \cong 1.096$ , and  $h_{c3} \cong 1.5960$ .
- Fig. 3- Average magnetization per unit cell (a) and the susceptibility in the field direction (b) as functions of the field, for  $n_A=2, n_B=3$ ,  $J=1, J_A=2, J_B=3$ , and  $h_A=h_B=h$ , at T=0. The critical fields are  $h_{c1}\cong 0.207, h_{c2}\cong 0.935, h_{c3}\cong 1.207, h_{c4}\cong 2.161$  and  $h_{c5}\cong 2.226$ .
- **Fig.4-** The real (a) and imaginary (b) parts of the correlation function  $\langle \tau_j^z(t)\tau_{j+1}^z(0)\rangle$ , as functions of the time, at T=0, for  $n_A=n_B=2$ ,  $J=1,\,J_A=2,\,J_B=3$ , and  $h=h_{1c}$  (plateau),  $h=h_{1c}+\varepsilon$ , with  $\varepsilon=0.01$  and 0.001.
- **Fig.5-** The same as in Fig. 4 for  $h = h_{3c}$  (plateaux),  $h = h_{3c} + \varepsilon$ , with  $\varepsilon = 0.01$  and 0.001.
- **Fig.6-** The real (a) and imaginary (b) parts of the correlation function  $\langle \tau_j^z(t)\tau_{j+1}^z(0)\rangle$ , as functions of the time, at T=0, for  $n_A=2, n_B=3$ ,  $J=1, J_A=2, J_B=3$ , and  $h=h_{1c}$  (plateau),  $h=h_{1c}-\varepsilon$ , with  $\varepsilon=0.01$  and 0.001.
- **Fig.7-** The same as in Fig. 6) for  $h=h_{3c}$  (plateaux),  $h=h_{3c}-\varepsilon$ , with  $\varepsilon=0.01$  and 0.001.
- **Fig.8-** The static correlation function  $\langle \tau_j^z \ \tau_{j+R}^z \rangle$  as a function of R (distance between cells), at T=0, for  $n_A=n_B=2,\ J=1,\ J_A=2,\ J_B=3,$  and for values of the field near and at the critical field.

- **Fig.9-** The static correlation function  $\langle \tau_j^z \ \tau_{j+R}^z \rangle$  as a function of R (distance between cells), at T=0, for  $n_A=2, n_B=3, J=1, J_A=2, J_B=3$ , and for values of the field near and at the critical field.
- **Fig.10-** Static susceptibility in the field direction,  $\chi_q^{zz}(0)$ , at T=0, as a function of the field for  $n_A=n_B=2,\ J=1,\ J_A=2,\ J_B=3,$  and  $h_A=h_B=h,$  and different values of q.
- **Fig.11-** Static susceptibility in the field direction,  $\chi_q^{zz}(0)$ , at T=0, as a function of the field for  $n_A=2, n_B=3, J=1, J_A=2, J_B=3$ , and  $h_A=h_B=h$ , and different values of q.
- **Fig.12-** The real (a) and imaginary parts of the dynamic susceptibility in the field direction,  $\chi_q^{zz}(\omega)$ , at T=0, as a function of frequency for,  $n_A=n_B=2, J=1,\ J_A=2, J_B=3,$  and h=0.693.
- **Fig.13-** The real (a) and imaginary parts of the dynamic susceptibility in the field direction,  $\chi_q^{zz}(\omega)$ , at T=0, as a function of frequency for,  $n_A=2, n_B=3,\ J=1,\ J_A=2, J_B=3,$  and h=0.2.

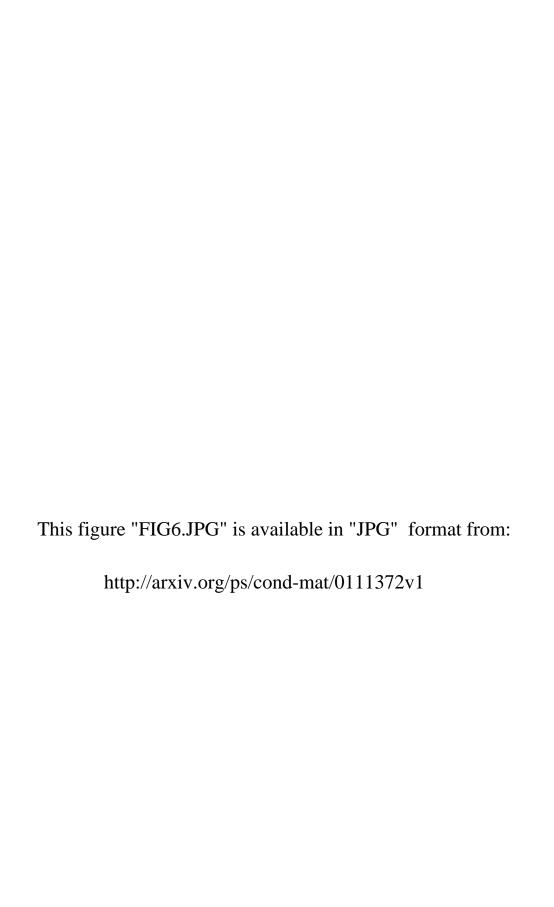
This figure "FIG1.JPG" is available in "JPG" format from:

This figure "FIG2.JPG" is available in "JPG" format from:

This figure "FIG3.JPG" is available in "JPG" format from:

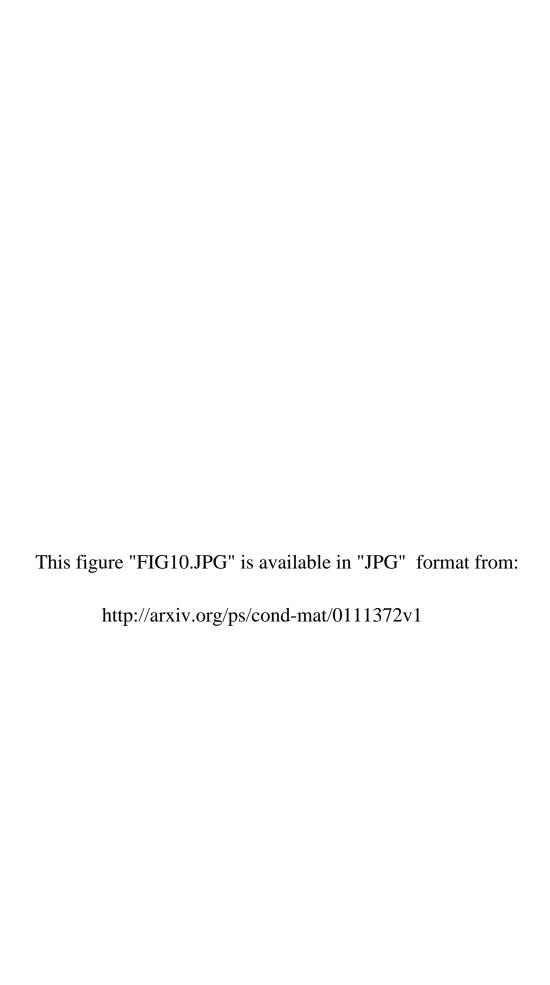
This figure "FIG4.JPG" is available in "JPG" format from:

This figure "FIG5.JPG" is available in "JPG" format from: http://arxiv.org/ps/cond-mat/0111372v1



This figure "FIG7.JPG" is available in "JPG" format from: http://arxiv.org/ps/cond-mat/0111372v1 This figure "FIG8.JPG" is available in "JPG" format from: http://arxiv.org/ps/cond-mat/0111372v1

This figure "FIG9.JPG" is available in "JPG" format from: http://arxiv.org/ps/cond-mat/0111372v1



This figure "FIG11.JPG" is available in "JPG" format from: http://arxiv.org/ps/cond-mat/0111372v1 This figure "FIG12.JPG" is available in "JPG" format from: http://arxiv.org/ps/cond-mat/0111372v1

This figure "FIG13.JPG" is available in "JPG" format from: http://arxiv.org/ps/cond-mat/0111372v1